Published in final edited form as:
Exp Neurol. 2006 February ; 197(2): 363–372. doi:10.1016/j.expneurol.2005.10.022.

Focal striatal dopamine may potentiate dyskinesias in parkinsonian monkeys

Krystof S. Bankiewicz[a,*], **Marcel Daadi**[a], **Philip Pivirotto**[a], **John Bringas**[a], **Laura Sanftner**[b], **Janet Cunningham**[a], **John R. Forsayeth**[a], and **Jamie L. Eberling**[c]

[a]Department of Neurological Surgery, University of California San Francisco, Mission Center Building 0555, 1855 Folsom Street, Room 230, San Francisco, CA 94103, USA

[b]Avigen Inc., Alameda, CA 94502, USA

[c]Department of Functional Imaging, Lawrence Berkeley National Laboratory, Berkeley, CA 94720, USA

Abstract

Striatal neurons convert L-dopa to dopamine (DA) following gene transfer of aromatic L-amino acid decarboxylase (AADC) via adeno-associated virus (AAV) in parkinsonian monkeys. We investigated whether AAV-AADC could reduce or eliminate L-dopa-induced dyskinesias (LIDs) and side effects in MPTP-treated monkeys. Five monkeys were made parkinsonian by bilateral MPTP lesions. The optimal therapeutic dose of L-dopa was determined using an acute dose response regimen. After 3 weeks of chronic L-dopa treatment, AAV-AADC or control vector was bilaterally injected into the striatum. Animals were assessed for 6 months with the same L-dopa dosing as presurgery as well as chronic oral L-dopa treatment. Presurgery LID was observed at doses greater than 5 mg/kg. The AAV-AADC-treated animals displayed an average 7.3-fold decrease in the therapeutic dose of L-dopa throughout the 6-month follow-up period. Only AAV-AADC-treated monkeys were susceptible to dyskinesias even at sub-clinical doses. Immunohistochemical analysis revealed well-delineated foci of AADC within the striatum. These results suggest that high levels of focal DA were generated in response to L-dopa administration and may be responsible for the exacerbation of dyskinesias. This may be similar to focal dopaminergic activity in PD patients that developed off-drug or "runaway" dyskinesias following fetal mesencephalic grafts.

Keywords

Dyskinesias; MPTP; AADC; AAV; L-dopa; Parkinson's disease; Monkey; Striatum; Dopamine

Introduction

Although L-dopa remains the mainstay of PD therapy, two-thirds of all patients develop motor complications within several years of initiation of therapy (Chase et al., 1993, Peppe et al., 1993), the most prominent of which are so-called L-dopa-induced dyskinesias (LID). Several patterns of dyskinetic movements have been identified: (i) peak-dose dyskinesias, (ii) dysphasic-dyskinesias, and (iii) end-of-dose dyskinesias (Marconi et al., 1994; Mones et al., 1971; Nutt, 1992; Obeso et al., 2000a,b; Olanow and Obeso, 2000). There is also the phenomenon of low-dose dyskinesias that pose particular clinical and treatment difficulties

*Corresponding author. Fax: +1 415 514 2777. kbank@itsa.ucsf.edu (K.S. Bankiewicz).

(Zimmerman et al., 1994). Patients with young-onset parkinsonism appear to be at the highest risk for developing debilitating dyskinesias (Chase et al., 1993; Mouradian et al., 1987; Nutt, 1992).

Another type of dyskinesia has recently been described in parkinsonian patients that received grafts of fetal mesencephalic tissue aimed at restoring DA innervation in the posterior putamen. These so-called “runaway dyskinesias” or off-drug (L-dopa) dyskinesias occurred in the absence of L-dopa medication (Freed et al., 2001; Ma et al., 2002; Olanow et al., 2003). These are considered to be an unexpected adverse event related to the fetal mesencephalon implantation procedure. Ma et al. (2002) demonstrated a significant increase in fluoro-dopa uptake determined by PET, strongly suggesting that fetal mesencephalic implants survived in the putamen and maintained the DA phenotype. Furthermore, postmortem analysis of PD patients that underwent a similar grafting procedure revealed surviving DA grafts within post-commissural putamen. However, these implants maintained a very focal morphology and had the appearance of DA “hotspots (Kordower and Sortwell, 2000; Olanow et al., 2001). It is likely that in these patients, off L-dopa dyskinesias were induced by (1) production of DA highly localized to the implant site rather than diffusely distributed throughout the relevant striatal area, (2) inability of the cells to form integrated connectivity with the host dopaminergic circuitry and (3) lack of regulation of the implanted fetal cells resulting in a continuous firing of the grafted dopaminergic cells.

The unanticipated adverse effects of grafting DA-producing tissue into the striatum of PD patients are worrisome for a number of reasons. First, numerous rodent and MPTP-treated monkey experiments in which fetal mesencephalon was grafted into the striatum did not predict these serious adverse effects. Second, none of the animal studies ever addressed the issue of potential interaction between grafted tissue and L-dopa administration, in hindsight an obvious clinical issue. Third, several promising treatment strategies, based on either stem cell technology or gene transfer technology, are now being investigated in animal models of PD and are contemplated for clinical application in the near future. Most of these are aimed at replacing a local deficiency of DA in the striatum, either by delivery of DA-producing cells or genes or by provision of trophic factors to provide local DA stimulation. Based on the observations that off-drug dyskinesias occurred in the two double-blind, controlled clinical trials of fetal DA-cell grafts, clinical application of these new and exciting technologies may offer limited clinical benefit, unless the mechanism underlying off L-dopa dyskinesias is understood. The present study may help to explain the effects of non-physiological and local delivery of DA in the striatum and its role in the generation of dyskinesias.

Over a number of years, we have developed a recombinant adeno-associated virus containing the cDNA encoding aromatic L-amino acid decarboxylase (AAV-AADC). Transduced with this vector, striatal neurons gain the ability to produce DA from exogenous L-dopa, a dopamine precursor. Briefly, expression of AADC in the striatum of parkinsonian rodents and monkeys greatly enhanced the efficacy of exogenously supplied L-dopa (Bankiewicz et al., 2000; Sanchez-Pernaute et al., 2001). In PD, it is primarily the loss of L-dopa conversion efficiency that underlies the progressive wearing off of L-dopa responsiveness. This blunting of L-dopa response may also underlie the appearance of motor complications, as the L-dopa response is impaired over several years of therapy. Such observations form the basis of a planned clinical investigation into AAV-AADC gene therapy for advanced PD.

During preclinical testing of this potential therapy in a monkey model of PD, we tested several different formulations of AAV-AADC. In one vector formulation that included an excess of empty AAV capsids produced by a column purification method, we observed reduction of AADC distribution associated with highly focal AADC expression determined by postmortem histochemical examination (Eberling et al., 2003). Diffuse expression of AADC is ordinarily

generated by convection-enhanced delivery (CED) of CsCl-purified vector (Bankiewicz et al., 2000). The association of the appearance of severe LID with focal delivery of AADC has led to the insight that highly focal delivery of AADC activity could be used to as a research tool to probe the neural mechanisms underlying dyskinesias.

Materials and methods

The experiments were performed on 5 non-naïve (see below) adult female Rhesus Macaques aged between 12 and 14 years in accordance with the NIH guidelines, NINDS and the University of California San Francisco Committee on Animal Research. The animals were housed separately in home cages in a temperature-controlled room and exposed to a 12-hour light-dark cycle. They were fed twice daily and water was provided ad libitum. All animals underwent MPTP lesioning 7 years prior to AAV-AADC gene transfer. Animals received clinical evaluations and in vivo imaging (both PET and MRI) prior to and after gene transfer. At the end of the study, animals were sacrificed, and histochemical analysis was performed. All of the procedures are described in detail below.

MPTP lesion/clinical evaluation

All monkeys were subcutaneously (s.c.) injected with 0.5–1.0 mg/kg of the neurotoxin MPTP-HCl (Sigma-Aldrich, dissolved in physiological saline) at 2–7 day intervals for 4–11 months until stable parkinsonian features were established. Animals displayed stable and advanced signs of PD for 7 years prior to AAV-AADC gene transfer. Clinical responses to L-dopa were evaluated throughout the post-MPTP period until animals were euthanized 8 years later. Both acute and chronic regimens were tested, and animals clearly responded to the drug, sometimes with dyskinesias at high doses of L-dopa. The most typical regimen of L-dopa administration in these animals involved adjustment of L-dopa to obtain maximal therapeutic effect with minimal side effects. As part of an earlier study, monkeys received unilateral administration of AAV-5 NTN (neuturin) with GDNF/bFGF/artemin protein co-infusion 4.5 years after the last MPTP dose. Animals were monitored clinically for 1.5 years with both L-dopa administration and FMT PET. No clinical improvement was detected, and no change in the FMT PET signal on the treated side was apparent 3 months after the treatment. One animal was euthanized, and the brain was examined histologically for NTN expression and increase of TH and AADC staining on the treated side. No NTN immunoreactivity was detected, and both sides of the brain remained symmetrical with no apparent changes in either TH or AADC staining, consistent with the PET results. Therefore, it was concluded that unilateral administration of AAV-5/NTN did not result in induction of NTN gene expression. On this basis, the remaining animals were deemed acceptable for use in the current study. Indeed, subsequent postmortem examination of these 5 animals did not reveal any NTN immunostaining, and endogenous dopaminergic innervation was symmetrical without any signs of increased DA fiber sprouting on the side of NTN administration.

Magnetic resonance imaging (MRI)

A baseline MRI was used to accurately place the cannula within the desired targeted structures and to co-register with PET images for anatomic localization. MRI was performed 6 to 8 months prior to gene transfer and within 48 h after surgery to confirm needle placement. During the scanning procedure, animals were sedated with Ketamine (Ketaset, 7 mg/kg, IM) and xylazine (Rompun, 3 mg/kg, IM) mixture. Each monkey was placed in the MRI-compatible stereotactic frame. The ear-bar and eye-bar measurements were recorded, and an intravenous line was established. Sixty coronal images (1 mm) were taken by a GE Sigma 1.5-T machine. MR images were T1-weighted and obtained in 3 planes with a spoil grass sequence, a repetition time (TR) = 700 ms, an echo time (TE) = 20 ms, and a flip angle of 30°. The field of view was 15 cm, with a 192 matrix and a 2NEX (number of averages per signal information). Scanning

time was approximately 20 min. Rostro-caudal and medio-lateral distribution of the targeted structure (e.g., caudate nucleus or putamen) was determined by use of the coronal MRI images. Surgical coordinates were determined from magnified coronal images (1.5×). One animal was scanned 7 days after AAV-AADC administration to determine acute effects of AAV-AADC delivery. Needle tracks were found at the precise sites in caudate nucleus and putamen and corresponded with anatomical regions of AADC gene transfer.

PET methods

PET was performed with a Siemens-CTI ECAT EXACT (model 951) 31-slice scanner prior to and 4 weeks after gene transfer. The AADC tracer, [^{18}F]fluoro-L-m-tyrosine (FMT), was produced with an on-site cyclotron, located directly adjacent to the scanner facility by a modification of the procedure described previously (Jordan et al., 1997). Immediately prior to PET imaging, monkeys were anesthetized with an i.m. injection of ketamine (15 mg/kg), intubated and placed on isoflurane anesthesia. The animals were kept normothermic with a heating blanket, hydrated with via a saphenous catheter, pO_2 monitored with an oximeter, and arterial blood pressure was monitored with an arterial catheter and transducer. The animals were placed in a stereotactic frame identical to the frame used for MRI. Images were acquired in the coronal plane. All animals were pretreated with an i.m. injection of benserazide (2 mg/kg), a peripheral decarboxylase inhibitor, 30 min before injection of the tracer. A 20-min transmission scan was obtained prior to the emission scan, in order to correct for photon attenuation, with a rotating 68 Ge source consisting of 3 rods of about 2 mCi/rod. Emission data were collected for 30 min beginning 45 min after the injection of approximately 5 mCi of FMT.

PET data analysis

The baseline PET and MRI data sets were co-registered, and regions of interest (ROIs) were drawn for the striatum and the cerebellum. ROIs were drawn directly on the MRI and subsequently mapped onto the PET images. The post-gene transfer PET data sets were co-registered to the baseline PET data sets and the baseline ROIs were mapped onto the post-gene transfer PET images. Radioactivity counts were determined for each ROI. Radioactivity count ratios were created using the cerebellum as a reference tissue. The cerebellum was selected as a reference region because FMT uptake there is negligible and should not change between baseline and post-treatment studies. Change scores for the count ratios were calculated as the percent change from baseline to post-AAV-AADC.

Neurological assessment

Behavioral assessments were performed in a blind fashion by a trained observer who had worked with these monkeys since MPTP administration. Clinical signs were evaluated with a clinical rating scale (CRS), by monitoring activity and by a staircase retrieval test.

Clinical rating scale (CRS)

The MPTP-induced parkinsonism and its relief following Sinemet-CR treatment were rated using the CRS for a maximal disability score of 42 in the following manner: 0 = normal, 1 = mild, 2 = moderate, 3 = severe, tremor right arm, tremor left arm, freezing, locomotion, fine motor skills right hand, fine motor skills left hand, bradykinesia right arm, bradykinesia left arm, posture, hypokinesia, balance, startle response, gross motor skills right hand and gross motor skills left hand. All animal testing was videotaped. Baseline CRS was collected pre and post-injection of the AAV-AADC or AAV-NULL. Weekly CRS were conducted on each animal 45 min after the AM dose of Sinemet-CR treatment. Dyskinesias and side effects were also rated and videotaped.

Acute L-dopa treatment

Animals with stable parkinsonian deficits were tested for acute response to L-dopa administration by i.m. injections of L-3,4,-dihydroxyphenylanine methyl ester (M-L-dopa) and benserazide to inhibit peripheral L-dopa decarboxylase. The following L-dopa doses were administered (0, 5, 10, 20, 40 mg/kg) in order to evaluate acute response to L-dopa. A wash-out period of 3 days was implemented between each dose. Clinical response and adverse effects were rated in response to each dose at 45 min. The dose that induced clear reduction of PD signs with minimal or no side effects was defined as the therapeutic dose (usually it is approximately 10–15 mg/kg of M-L-dopa, i.m.). After AAV-AADC infusion, the animals received weekly injections of increasing doses of L-dopa: 1.5, 2.5, 5, 10, 20, 30 mg/ml combined with benserazide (2 mg/kg), and dyskinesia was scored. The dyskinesia scores of animals treated with AAV-AADC were averaged for each L-dopa dose before and after surgery and reported as mean ± SEM.

Chronic L-dopa treatment

Sinemet CR was given BID for 5 weeks. The therapeutic dose of L-dopa was determined for each monkey and adjusted to one of the following doses: 50/200 mg, 25/100 mg or 12.5/50 mg L-dopa/Carbidopa to avoid or minimize dyskinesias or other adverse effects of L-dopa administration.

Dyskinesia assessment

The severity of dyskinesias was scored for different segments of the animal's body including face, trunk, arms and legs on a scale from 0 to 3, with 0 = absent, 1 = mild, 2 = moderate, 3 = severe. The severity of the rating is based on the frequency and amplitude of the abnormal movement. The dyskinetic score was obtained by adding the scores of all body segments for a maximal score of 18.

Assessment of side effects

The rating of side effects was based on the duration, frequency, intensity and interference with daily animal activities of any post-treatment manifestation. These side effects were rated as follows: Absent = 0, Mild = 1: transient and includes hyperactivity, distractibility, aggression, scratching, yawning, vocalizations, tooth grinding and over grooming. Moderate = 2: sustained and frequent manifestations including hyperactivity, diarrhea, unusual postures such as lying down, aggression. Severe = 3: intense and frequent manifestations including hyperactivity, vomiting, diarrhea, psychiatric disturbances, abnormal postures, aggression and self-mutilation.

Videotaping protocol

A Standard Operating Procedure (SOP) was developed for videotaping monkeys at different stages of the experiment. Arm retrieval test was always videotaped and data collected from the tapes. Clinical rating was videotaped at least once a month. This assures that permanent clinical record can be reviewed once secondary measures were in place.

Stereotactic surgery

The delivery system consisted of 3 components: (i) sterile infusion cannula, (ii) sterile loading line for rAAV vector, (iii) non-sterile infusion line containing olive oil. The step-design infusion cannula is composed of a 27-gauge needle (OD: 0.3 in.; ID: 0.06 in.; Terumo Corp., Elkton, MD) fitted with fused silica (OD: 0.16 in.; ID: 0.008 in.; Polimicro Technologies, Phoenix, AZ) and placed in Teflon tubing (ID: 0.03 in.; Upchurch Scientific, Seattle, WA) such that the distal tip of the silica extend approximately 5 mm out of the tubing. The needle

was secured into the tubing using superglue and the whole infusion line was checked to prevent leaking prior to use. At the proximal end of the tubing, a Tefzel fitting and ferrule were attached to connect the adjacent loading line. Loading and infusion lines consisted of 50-cm sections of Teflon tubing (OD: 0.062 in.; ID: 0.03 in.) fitted with Tefzel 1/16 in. ferruled, unions, and made Luer-lock adapters (Upchurch Scientific, Oak harbor, WA) at the distal ends. The sterile loading lines accommodated up to 1 ml and were primed with PBS/F68 prior to use to decrease binding of the viral particles to the tubing.

Recombinant AAV vector infusion

For each hemisphere, 3 cannulae were attached into a block mounted into the stereotactic frame that allows for adjustment of the cannulae according to MRI measurements. One cannula was placed in the caudate nucleus and two in the putamen on each side. Total volume of 33 μl of column-purified vector was delivered at each site (×3 sites per hemisphere × 2 hemispheres = 198 μl total volume per animal) with 1×10^{12} total vector genomes (vg) (or 5×10^{12} total AAV particles) per animal of either AAV-AADC ($n = 3$) or AAV-NULL ($n = 2$).

AAV vector production

The HEK 293 cell line was cultured in complete DMEM (BioWhittaker) containing 4.5 g/l glucose, 10% heat-inactivated fetal calf serum (FCS) and 2 mM glutamine at 37°C at 5% CO_2. Following cell expansion in T-flasks, fifty roller bottles were seeded with 2×10^7 cells each and grown for 3 days to 70–80% confluency (approximately 1×10^8 cells per bottle) prior to transfection. The HEK 293 cells were transfected by the calcium phosphate method with 150 μg of each of the following 3 plasmids per roller bottle: AAV-AADC plasmid (containing AADC under the control of a CMV promoter), the AAV helper plasmid (pHLP19, containing the AAV rep and cap genes) and the adenovirus helper plasmid (pladeno-5, previously known as pVAE2AE4-2 and composed of the E2A, E4, and VA RNA genes derived from purified adenovirus-2). Twenty-four hours after transfection, the medium was exchanged, replacing the transfection mixture with serum-free growth medium. The cells were incubated for an additional 2 days to allow vector amplification and then harvested, homogenized by micro-fluidization and clarified by sequential filtration through 0.65 and 0.2 μm depth filters. Sequential cation and anion exchange column chromatography steps further purified the AAV-AADC vector. The purified vector, recovered from the second column was concentrated and diafiltered by tangential flow filtration, and finally formulated with 0.001% Poloxamer 188. Formulated vector was filtered through a 0.22-μm disc filter and aseptically dispensed into polypropylene cryovials and stored at −80°C. The titer of the purified AAV-AADC vector (5×10^{12} vg/ml) was determined by real-time quantitative PCR analysis. Unlike traditional CsCl gradient purification, column purification methods do not remove viral “empty capsids”. The vector preparations contained empty AAV capsid particles at a ratio of 4:1 over “full” or vector genome-containing capsids, as determined by AAV capsid ELISA.

Construction of AAV plasmids

A 1.5-kb BamHI/PvuII cDNA containing the coding sequence for human AADC (the generous gift of Dr. Keiya Ozawa, Jichi Medical School, Tochigi, Japan) was cloned into the AAV expression casette pV4.1c at BamHI/HindII sites. The expression cassette contained a CMV promoter, a chimeric intron composed of a CMV splice donor and a human globin splice acceptor site, human growth hormone polyadenylation sequence and flanking AAV ITRs (inverted terminal repeats). The AAV-AADC plasmid was similar to that described previously (Bankiewicz et al., 2000) except that 1.3 kb of bacterial spacer sequence was removed. The AAV-NULL vector is promoterless construct that contains the β-galactosidase gene, Neo gene, and flanking AAV2 ITRs.

Histochemistry

Tissue preparation—Monkeys were sacrificed 6 months after gene transfer. Monkeys were tranquilized with ketamine (10 mg/kg, i.m.), intubated and anesthetized with nembutal (25 mg/kg, iv). They were then perfused sequentially with warm (100 ml) and ice-cold saline (100 ml) and formalin (500 ml). The brains were removed, placed in a brain matrix and sectioned coronally into 6-mm slices. Brain slices were washed in PBS for 12 h, equilibrated in an ascending sucrose gradient (10–20–30%) and frozen. The formalin-fixed brain slices were cut into 30-μm thick coronal sections in a cryostat. Sections were collected in series starting at the rostral tip of the caudate nucleus and extending caudally through the midbrain. Each section was stored in cyroprotectant at −70°C.

Immunocytochemistry—Frozen coronal sections (40 μm through the striatum and SN) were cut on a sliding microtome, and stored in cryoprotective solution at −20°C. Immunocytochemistry by the Nickel-enhanced biotin–avidin–peroxidase method were carried out for TH, GFAP, NeuN and AADC. For immunofluorescent detection, the indirect method was used and bound antibody detected by FITC-, AMCA- or TRITC-conjugated-IgG (1:200). Positive and negative controls were included in each run. Immuno-peroxidase and immuno-fluorescent staining of tissue sections were performed on selected serial sections for NeuN, GFAP and hAADC.

Results

Chronic and repeated systemic administrations of MPTP resulted in a bilateral parkinsonian deficit in all the animals. The clinical deficits included severe bradykinesia, freezing, tremor, akinesia, postural instability, lack of vocalization, decreased startle response and reduced grooming that was stable for 5–7 years prior to gene transfer. Similar to the human disease, therapeutic responses to L-dopa administration varied between the animals but remained consistent for each subject during the pregene transfer testing period.

Histochemical findings

Immunohistochemical analysis of AADC expression in the 3 PD monkeys treated with AAV-AADC shows highly concentrated and focal AADC expression in the putamen and caudate (Fig. 1–Fig. 3). This pattern of expression was associated in each case with the appearance of LID (see below). AADC expression was restricted to medium spiny neurons (expressing D1 and D2 receptors). Thus, L-dopa administration (L-dopa is converted DA by AADC expressing cells) results in activation of DA receptor-bearing cells only within a restricted region of the striatum.

PET-FMT findings

AADC activity was determined prior to, and approximately 4 weeks after, AAV-AADC gene transfer using PET. The two AAV-NULL animals showed little change in the PET ratios bilaterally from baseline (Fig. 4). Whereas two of the AAV-AADC-treated animals showed small bilateral increases over baseline (Fig. 1, Fig. 2 and Fig. 4), the third monkey (Fig. 3 and Fig. 4) showed a more prominent increase in FMT signal bilaterally. Similarly, AADC expression in the striatum of this animal was the most pronounced of all of the AADC-treated animals (Fig. 3), nevertheless remaining very focal. The threshold for AADC detection with PET is diminished with very focal AADC expression as shown by the small differences between the two AAV-NULL animals and two of the AAV-AADC animals. The between scan variability inherent in this method further reduces the sensitivity for detecting small changes produced by very focal AADC distribution, as confirmed by the histochemical analysis.

Clinical response to acute and chronic L-dopa administration

L-dopa administration was clinically effective in all of the monkeys with reduction of many PD signs, i.e., lower clinical score. Acute administration of several doses of L-dopa/benserazide showed dose-dependent clinical effects with induction of clear adverse side effects at the high doses. These adverse effects included hyperactivity, stereotypic behavior and dyskinesias that were limited to lower and upper extremities and trunk. Occasional face grimacing and tongue dyskinesias were also observed. A chronic regimen of L-dopa (Sinemet CR rather than L-dopa/beserazide was used in chronic administration) resulted in measurable clinical improvement that was associated with adverse side effects. L-dopa-induced dyskinesias were present as well but typically they were induced at the initial phases of chronic L-dopa treatment.

The therapeutic dose of L-dopa in this study ranged from 10 to 30 mg/kg. Subsequent to gene transfer, the response of animals to acute (Fig. 5) and chronic administration of L-dopa (Fig. 6) was tested at 2 and 4 months, respectively. Acute challenge with L-dopa induced maximal clinical response in AADC-treated animals at doses lower than those seen before gene transfer, suggesting more efficient conversion of L-dopa to DA (Fig. 5A). However, the onset and magnitude of dyskinesias were also amplified (Fig. 5B). Within 24 h of the initiation of chronic administration of L-dopa, dyskinesias appeared only in the AADC-treated animals (Figs. 6A and B). In addition to dyskinesias, these monkeys displayed hyperactivity and apparent hallucinations. The overall clinical score was improved at week 1, and animals were kept at the same dose of L-dopa (Sinemet 100 mg BID) for an additional week. Clinical benefit of L-dopa administration persisted but was associated with the same magnitude of dyskinesias. The L-dopa dose was reduced for all the AADC-treated monkeys on a weekly basis to alleviate dyskinesias; nonetheless, all 3 remained dyskinetic for the duration of L-dopa administration (Fig. 6B). Once L-dopa was discontinued, dyskinesias disappeared within 24 h.

In a parallel experiment (Figs. 6C and D), MPTP-treated monkeys, in which AAV-AADC was diffusely rather than focally distributed in caudate nucleus and putamen (see Bankiewicz et al., 2000 for methodology), were subjected to chronic administration of Sinemet (Fig. 6D). In these animals L-dopa administration did not induce dyskinesias, regardless of the dose used. Control animals showed good clinical improvement in response to chronic L-dopa administration, and no dyskinesias were present in response to the same dose of L-dopa that was given to AAV-AADC-treated animals. The only side effect of L-dopa administration seen in these monkeys was hyperactivity that persisted until the dose of L-dopa was decreased by half (Figs. 6C and D). These results strongly suggest that focal DA stimulation in the striatum is associated with LID and non-motor adverse effects (possibly due to caudate nucleus stimulation).

Discussion

The AAV-AADC-treated animals showed focal bilateral increases in FMT signal that corresponded with immunohistochemical findings of highly concentrated and focal AADC expression in the caudate and putamen. This focal pattern of expression was associated with LID in all of the AAV-AADC-treated animals, even at low doses of L-dopa. These findings suggest a model for exploring the mechanisms underlying LID, as discussed below.

In monkeys with MPTP-induced parkinsonism, it has been shown that extensive dopamine depletion leads to an up-regulation of D2 receptors, whereas D1 receptors are down-regulated (Alexander et al., 1991). Walters et al. (1987) found that both D1 and D2 activation are necessary for the development of dyskinesias, an observation that has been confirmed by another group (Bedard et al., 1993). Graham (1992) has proposed that, in the MPTP-lesioned monkey, chronic treatment with L-dopa normalizes the D2 receptor up-regulation after DA depletion. However, similar to the findings in rats, D1 receptor down-regulation is exaggerated.

It has also been demonstrated in monkeys that there is a prolonged dopamine receptor occupancy, reflecting altered intracerebral L-dopa/dopamine pharmacokinetics (Hammerstad et al., 1990). This has also been demonstrated in severe cases of human parkinsonism in patients with indwelling ventricular shunts. The extent of the lesion of the nigrostriatal pathway appears to correlate with the development of dyskinesias; that is, severely lesioned animals require shorter duration of L-dopa treatment and lower doses to produce dyskinesia (Boyce et al., 1990; Di Monte et al., 2000; Schneider, 1989). The severity of MPTP-induced PD signs and short timing of MPTP administration have also been recently indicated in the development of LID (Schneider et al., 2003).

Our results lead us to the conclusion that focal DA stimulation of the striatum is a likely result of the abnormally focal distribution of AADC expression in these animals. This focal DA synthesis capacity in turn leads to severe dyskinesias in response to L-dopa administration. Although, in this study, we did not evaluate focal dopamine-producing cell implants (Steece-Collier et al., 2003), we believe that our results have direct relevance to the pathophysiology of "run away" dyskinesias seen in PD subjects after fetal cell grafting. It is conceivable that in the patients that developed "off L-dopa" dyskinesias, the production of DA by the graft was highly localized to the implant site rather than diffusely distributed throughout the relevant striatal region. The inability of the grafted cells to form integrated connectivity with the host dopaminergic circuitry in the basal ganglia, and lack of regulation of the implanted fetal cells, could have resulted in a continuous firing pattern of the grafted dopaminergic cells and non-physiological over-activation of a fraction of basal ganglia circuitry. In this experiment, it is critical to note that AAV-AADC-transduced striatal cells are otherwise integrated into the basal ganglia circuitry. Thus, L-dopa administration results in immediate DA-dependent activation of only a focal region of the striatum.

In the present case, one focal site in the caudate nucleus and 2 sites in the putamen on each side of the brain were targeted. It is impossible to deduce from our current results whether all 3 sites cooperate to trigger dyskinesia or whether only a single site was responsible. However, it is conceivable that the posterior putamen (one of our sites) may be directly linked to generation of dyskinesias, since studies in humans show that the placement of dopaminergic cells in this region triggered severe dyskinesias (Freed et al., 2001; Ma et al., 2002; Olanow et al., 2003). Also, in intriguing studies in which kainic acid was used to create reasonably localized damage to basal ganglionic structures, dyskinesias resulted only from lesions in the posterior putamen and not in caudate nucleus or anterior putamen (Burns et al., 1995).

Previous studies done in our laboratory found that the distribution of AADC in a diffuse fashion did not result in LIDs, strongly indicating a role for focal dopamine production in the exacerbation of LIDs. Our ability to express AADC in specific regions of the striatum provides us with an exceptional tool for investigating effects of local DA stimulation on basal ganglia circuitry. Taken as a whole, our findings suggest that DA replacement strategies in human subjects must avoid the creation of focal aberrations in dopaminergic tone and further that such local disparities in dopaminergic activity may underlie the development of LID seen so commonly in PD.

Acknowledgments

The authors thank Dr. Michael Aminoff for the critical review of the manuscript. Funding for this work was provided by NINDS IRP and R21 NS43707 grants and Avigen, Inc., Alameda, CA, to KSB.

References

Alexander GM, Brainard DL, Gordon SW, Hichens M, Grothusen JR, Schwartzman RJ. Dopamine receptor changes in untreated and (+)-PHNO-treated MPTP parkinsonian primates. Brain Res 1991;547:181–189. [PubMed: 1679365]

Bankiewicz KS, Eberling JL, Kohutnicka M, Jagust W, Pivirotto P, Bringas J, Cunningham J, Budinger TF, Harvey-White J. Convection-enhanced delivery of AAV vector in parkinsonian monkeys; in vivo detection of gene expression and restoration of dopaminergic function using pro-drug approach. Exp. Neurol 2000;164:2–14. [PubMed: 10877910]

Bedard PJ, Gomez-Mancilla B, Blanchette P, Gagnon C, Falardeau P, DiPaolo T. Role of selective D1 and D2 agonists in inducing dyskinesia in drug-naive MPTP monkeys. Adv. Neurol 1993;60:113–118. [PubMed: 8093573]

Boyce S, Clarke CE, Luquin R, Peggs D, Robertson RG, Mitchell IJ, Sambrook MA, Crossman AR. Induction of chorea and dystonia in parkinsonian primates. Mov. Disord 1990;5:3–7. [PubMed: 2296255]

Burns LH, Pakzaban P, Deacon TW, Brownell AL, Tatter SB, Jenkins BG, Isacson O. Selective putaminal excitotoxic lesions in non-human primates model the movement disorder of Huntington disease. Neuroscience 1995;64:1007–1017. [PubMed: 7753372]

Chase T, Engber T, Mouradian M. Striatal dopamine receptive system changes and motor response complications in l-dopa-treated patients with advance disease. Adv. Neurol 1993;60:181–185. [PubMed: 8420133]

Di Monte D, McCormack A, Petzinger G, Janson A, Quik M, Langston J. Relationship among nigrostriatal denervation, parkinsonism and dyskinesias in the MPTP primate model. Mov. Disord 2000;15:459–466. [PubMed: 10830409]

Eberling JL, Cunningham J, Pivirotto P, Bringas J, Daadi MM, Bankiewicz KS. In vivo PET imaging of gene expression in parkinsonian monkeys. Mol. Ther 2003;8:873–875. [PubMed: 14664788]

Freed CR, Greene PE, Breeze RE, Tsai WY, DuMouchel W, Kao R, Dillon S, Winfield H, Culver S, Trojanowski JQ, Eidelberg D, Fahn S. Transplantation of embryonic dopamine neurons for severe Parkinson's disease. N. Engl. J. Med 2001;344:710–719. [PubMed: 11236774]

Graham WCSM, Crossman AR. Differential effect of chronic dopaminergic treatment on dopamine D-1 and D-2 receptors in the monkey brain in MPTP-induced parkinsonism. Brain Res 1992;602:290–303. [PubMed: 8095431]

Hammerstad J, Woodward W, Gliessman P, Boucher B, Nutt J. l-dopa pharmacokinetics in plasma and cisternal and lumbar cerebrospinal fluid of monkeys. Ann. Neurol 1990;27:495–499. [PubMed: 2360790]

Jordan S, Eberling JL, Bankiewicz KS, Rosenberg D, Coxson PG, VanBrocklin HF, O'Neil JP, Emborg ME, Jagust WJ. 6-[^{18}F] fluoro-l-m-tyrosine: metabolism, positron emission tomography kinetics, and 1-methyl-4-phenyl-1,2,3,6-tetrahydropyridine lesions in primates. Brain Res 1997;750:264–276. [PubMed: 9098552]

Kordower JH, Sortwell CE. Neuropathology of fetal nigra transplants for Parkinson's disease. Prog. Brain Res 2000;127:333–344. [PubMed: 11142034]

Ma Y, Feigin A, Dhawan V, Fukuda M, Shi Q, Greene P, Breeze R, Fahn S, Freed C, Eidelberg D. Dyskinesia after fetal cell transplantation for parkinsonism: a PET study. Ann. Neurol 2002;52:628–634. [PubMed: 12402261]

Marconi R, Lefebvre-Caparros D, Bonnet A-M, Vidailhet M, Dubois B, Agid Y. Levodopa-induced dyskinesias in Parkinson's disease phenomenology and pathophysiology. Mov. Disord 1994;9:2–12. [PubMed: 8139601]

Mones RJ, Elizan TS, Siegel GJ. Analysis of l-dopa induced dyskinesias in 51 patients with Parkinsonism. J. Neurol., Neurosurg. Psychiatry 1971;34:668–673. [PubMed: 5158780]

Mouradian MM, Juncos JL, Fabbrini G, Chase TN. Motor fluctuations in Parkinson's disease: pathogenic and therapeutic studies. Ann. Neurol 1987;22:475–479. [PubMed: 3435068]

Nutt, J. Dyskinesia induced by levodopa and dopamine agonists in patients with Parkinson's disease. In: Lang, A.; Weiner, W., editors. Drug-Induced Movement Disorders. Futura: Mount Kisko; 1992. p. 281-314.

Obeso JA, Olanow CW, Nutt JG. Levodopa motor complications in Parkinson's disease. Trends Neurosci 2000a;23:S2–S7. [PubMed: 11052214]

Obeso JA, Rodriguez-Oroz MC, Rodriguez M, Lanciego JL, Artieda J, Gonzalo N, Olanow CW. Pathophysiology of the basal ganglia in Parkinson's disease. Trends Neurosci 2000b;23:S8–S19. [PubMed: 11052215]

Olanow CW, Obeso JA. Preventing levodopa-induced dyskinesias. Ann. Neurol 2000;47:S167–S176. [PubMed: 10762145](discussion S176-168).

Olanow CW, Freeman T, Kordower J. Transplantation of embryonic dopamine neurons for severe Parkinson's disease. N. Engl. J. Med 2001;345:146. [PubMed: 11450669](author reply 147)

Olanow CW, Goetz CG, Kordower JH, Stoessl AJ, Sossi V, Brin MF, Shannon KM, Nauert GM, Perl DP, Godbold J, Freeman TB. A double-blind controlled trial of bilateral fetal nigral transplantation in Parkinson's disease. Ann. Neurol 2003;54:403–414. [PubMed: 12953276]

Peppe A, Dambrosia J, Chase T. Risk factor for motor response complications in l-dopa-treated Parkinsonian patients. Adv. Neurol 1993;60:698–702. [PubMed: 8420213]

Sanchez-Pernaute R, Harvey-White J, Cunningham J, Bankiewicz KS. Functional effect of adeno-associated virus mediated gene transfer of aromatic l-amino acid decarboxylase into the striatum of 6-OHDA-lesioned rats. Mol. Ther 2001;4:324–330. [PubMed: 11592835]

Schneider J. Levodopa-induced dyskinesias in parkinsonian monkeys: relationship to extent of nigrostriatal damage. Pharmacol. Biochem. Behav 1999;34:193–196. [PubMed: 2576311]

Schneider JS, Gonczi H, Decamp E. Development of levodopa-induced dyskinesias in parkinsonian monkeys may depend upon rate of symptom onset and/or duration of symptoms. Brain Res 2003;990:38–44. [PubMed: 14568327]

Steece-Collier K, Collier TJ, Danielson PD, Kurlan R, Yurek DM, Sladek JR Jr. Embryonic mesencephalic grafts increase levodopa-induced forelimb hyperkinesia in parkinsonian rats. Mov. Disord 2003;18:1442–1454. [PubMed: 14673880]

Walters J, Bergstrom D, Carlson J, Chase T. D1 dopamine receptor activation required for postsynaptic expression of D2 agonist effects. Science 1987;236:719–722. [PubMed: 2953072]

Zimmerman T, Sage J, Lang A, Mark M. Severe evening dyskinesias in advanced Parkinson's disease: clinical description, relation to plasma levodopa, and treatment. Mov. Disord 1994;9:173–177. [PubMed: 8196678]

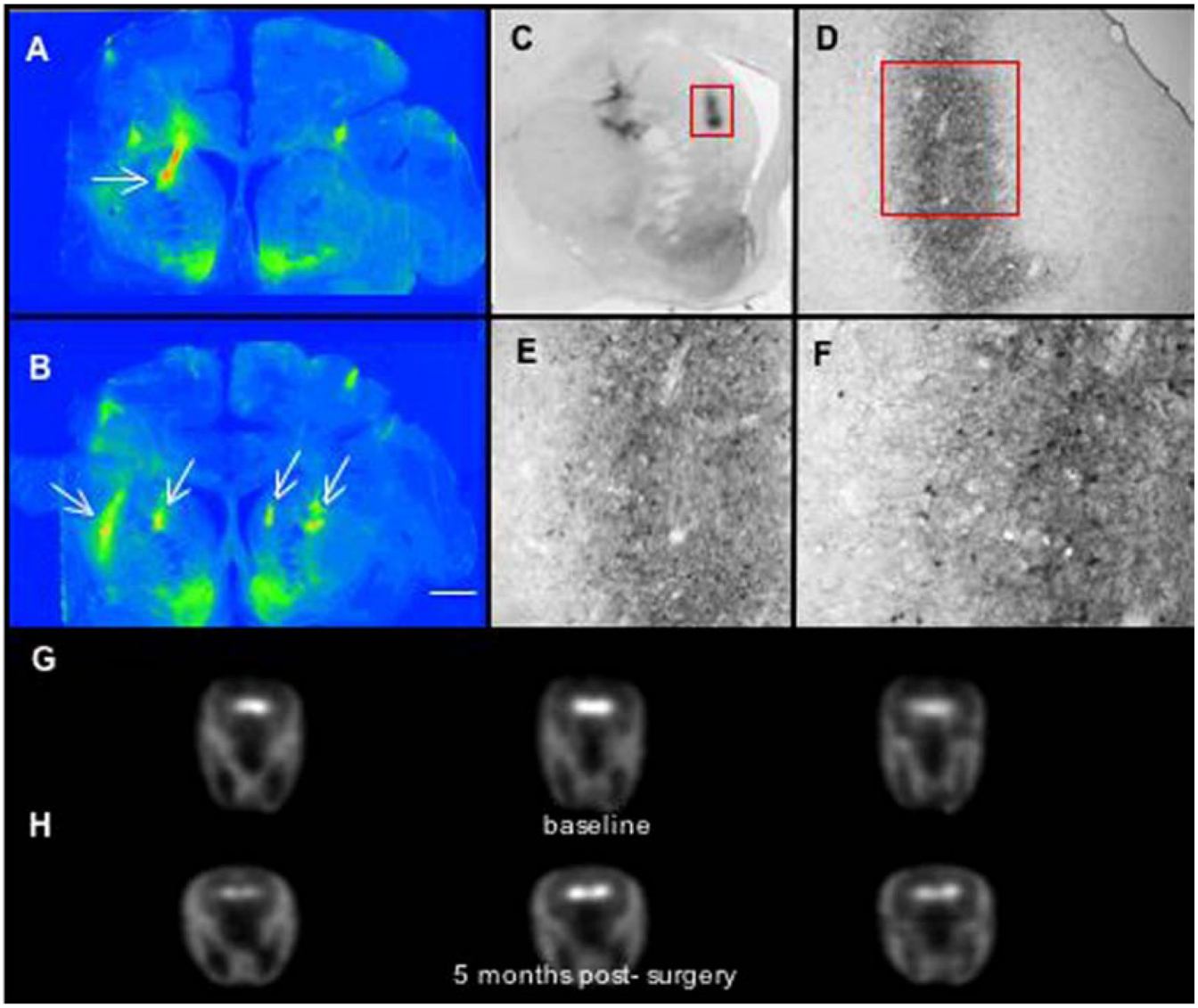

Fig. 1.
Immunostaining and PET imaging of AAV-AADC-treated monkey (RQ 1065).

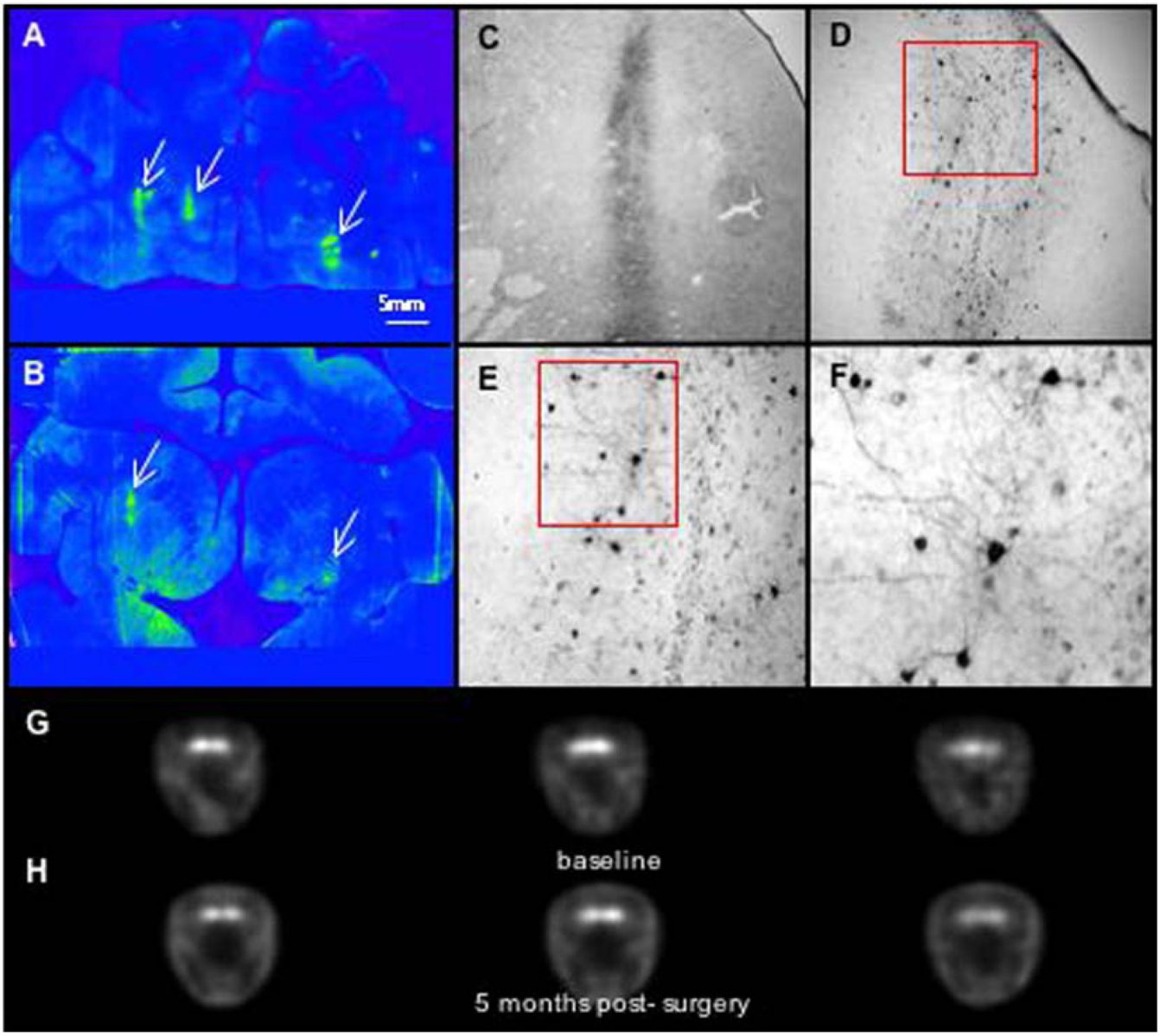

Fig. 2.
Immunostaining and PET imaging of AAV-AADC-treated monkey (RQ 1077).

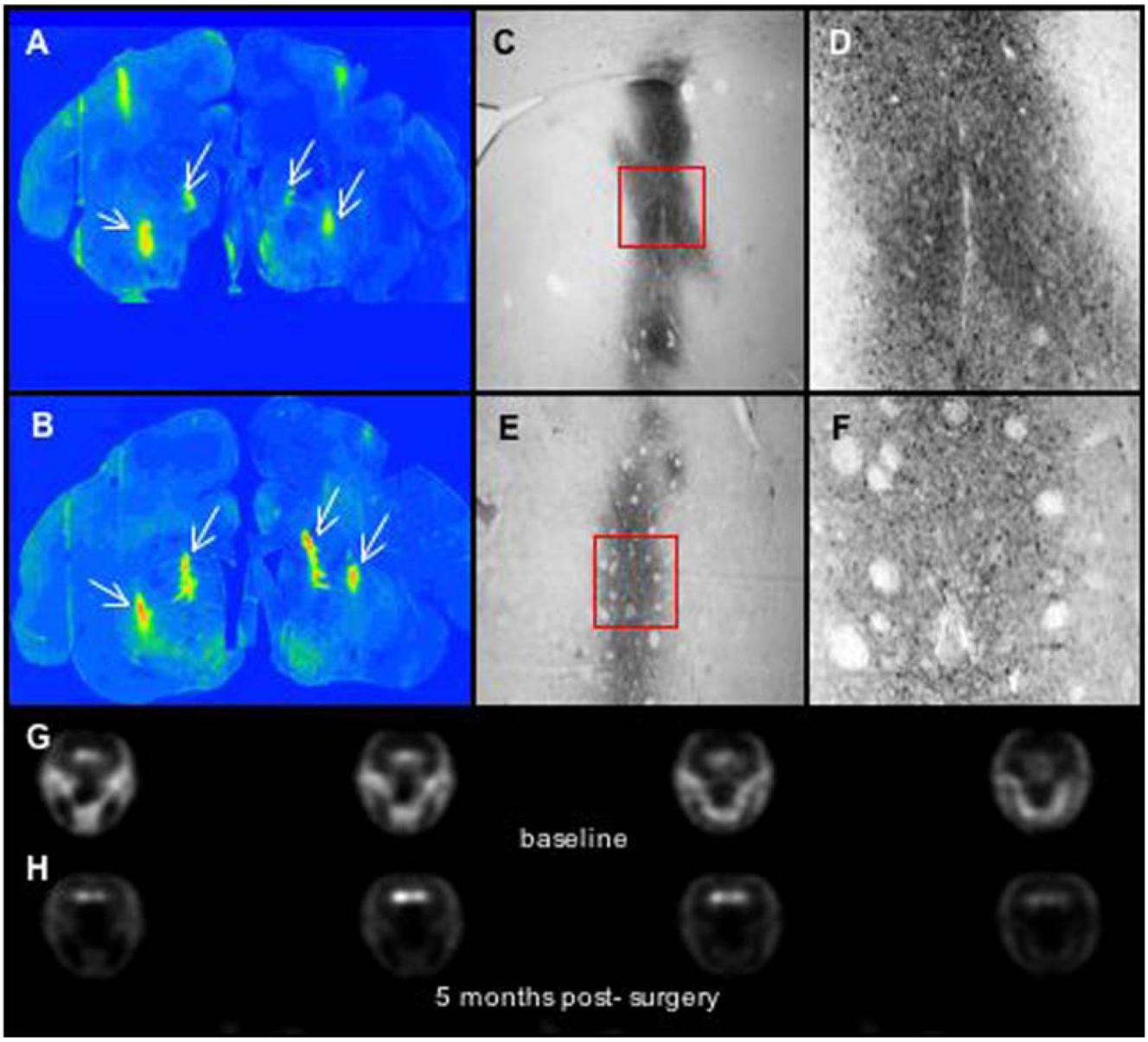

Fig. 3.

Immunostaining and PET imaging of AAV-AADC-treated monkey (TO11). (A, B) Low power photomicrographs of AADC-IR with focal AADC expression. One site in the caudate nucleus and 2 sites in the putamen were targeted bilaterally. Note very low levels of AADC in the striatum with exception of nucleus accumbens and focal regions (as indicated by arrows) of AADC gene transfer 6 months following AAV-AADC administration. (C–F) High power photomicrographs of the AADC-transduced regions in the caudate as shown in panels A and B. AADC expression is restricted to medium spiny neurons (expressing D1 and D2 receptors). Also note the very short distance of AADC-IR fibers extending from the focus of AADC transduction. Local DA production by AADC-expressing striatal neurons in response to L-dopa administration most likely represents focal DA production. *L-dopa administration in these monkeys resulted in significant induction of dyskinesias* (see clinical rating figures). (G–H) 6-[^{18}F]fluoro-L-m-tyrosine (FMT) positron emission tomography (PET) before and approximately 4 weeks after AAV-AADC gene transfer. Three brain levels (anterior to

posterior) are shown for baseline and post-gene transfer. Low levels of FMT activity were seen following AADC gene transfer due to limited expression of AADC in the striatum. Scale bar: 5 mm.

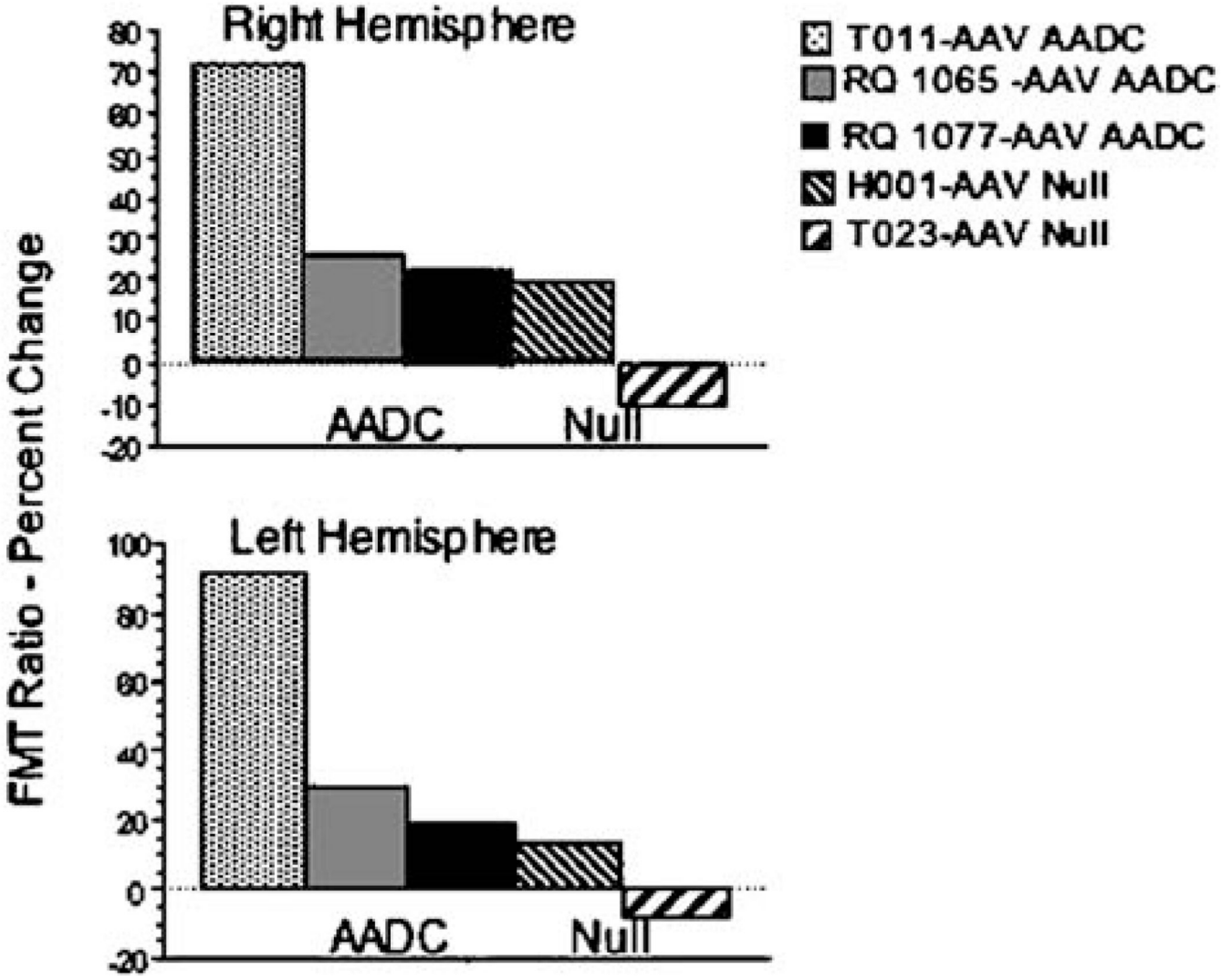

Fig. 4.

PET imaging-percent change from baseline. Quantification of AADC activity. Data represent %change in FMT striatal uptake ratios between baseline and post-AAV scan for each monkey in right and left hemispheres. The two AAV-NULL animals showed little change in PET ratios from baseline. Two of the AAV-AADC-treated animals showed small bilateral increases and the third animal showed a more prominent increase bilaterally.

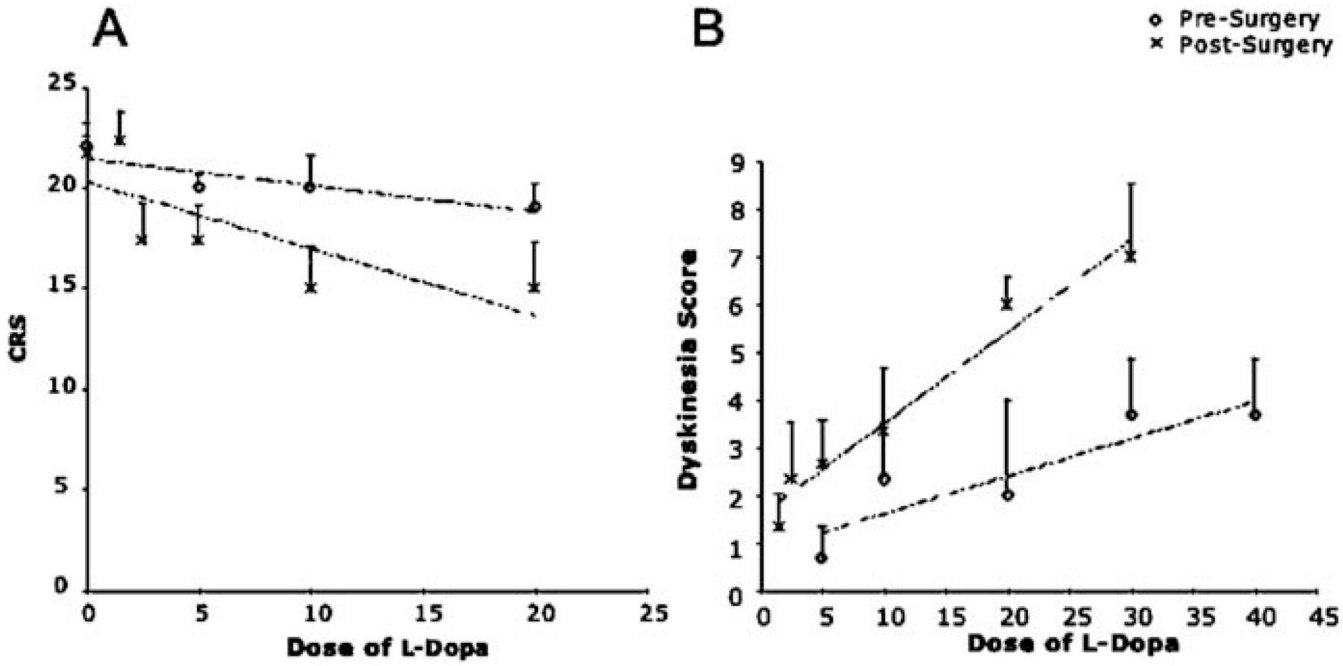

Fig. 5.

Response of AAV-AADC-treated monkeys to acute L-dopa. (A) Clinical responses to acute administration of L-dopa (0, 5, 10, 20 mg/kg) were rated at 45 min. A 3-day wash-out was implemented between each dose. Improved L-dopa response was seen by reduction of CRS scores after AADC gene transfer. However, it was associated with significantly elevated dyskinesias as shown in panel B. (B) The animals received weekly injections of increasing doses of L-dopa: 1.5, 2.5, 5, 10, 20, 30 mg/ml combined with the decarboxylase inhibitor benserazide (2 mg/kg) and dyskinesias were scored. The dyskinesia scores of animals treated with AAV-AADC were averaged for each L-dopa dose before and after surgery and are reported as mean ± SEM.

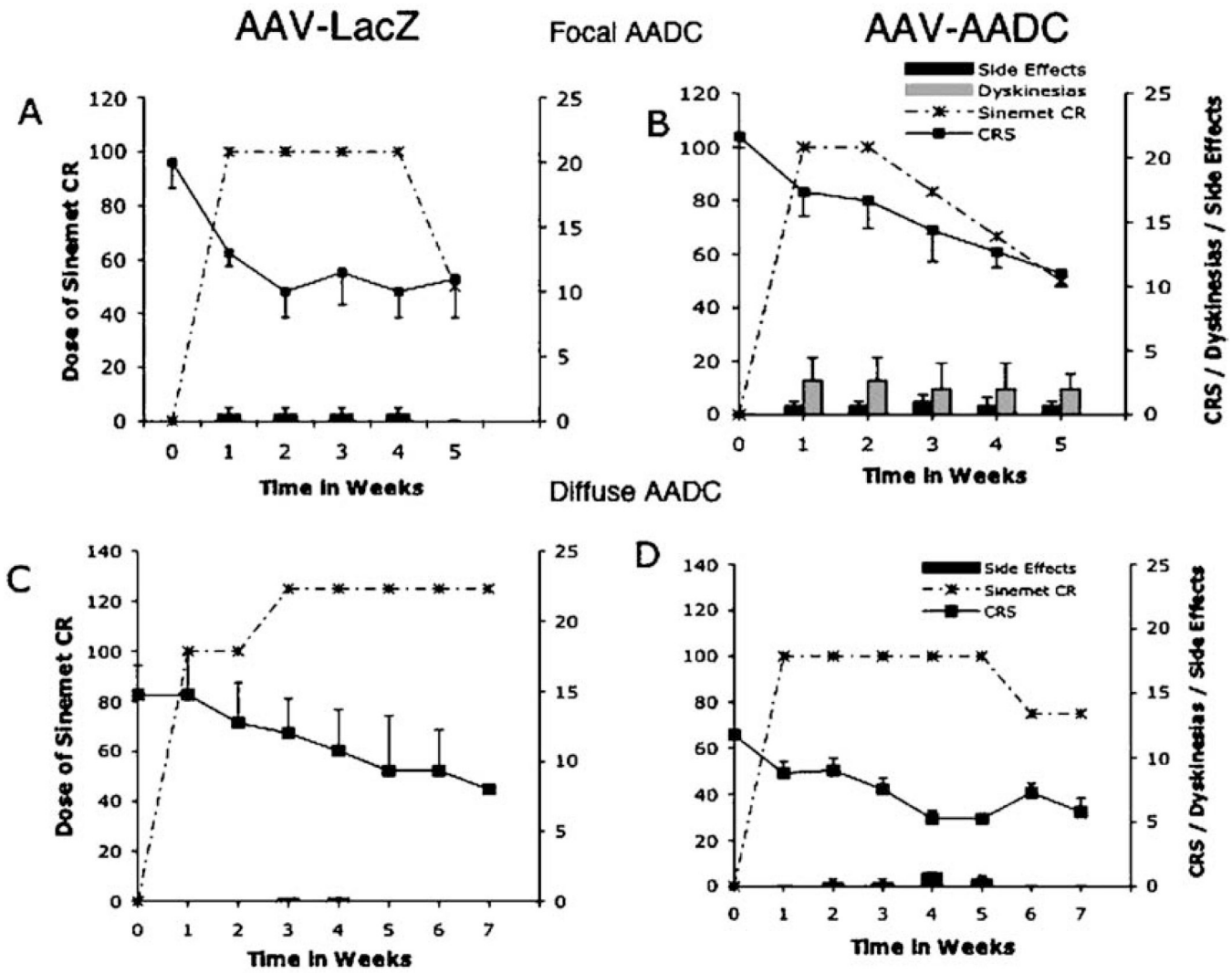

Fig. 6.

Response of AAV-AADC-treated and control monkeys to chronic L-dopa. Sinemet CR was given BID for 5 weeks. The therapeutic dose of L-dopa was determined for each monkey and adjusted to one of the following doses: 50/200 mg, 25/100 mg, 12.5/50 mg (L-dopa/Carbidopa) to avoid or minimize dyskinesias or other adverse effects of L-dopa administration. (A and B) Clinical improvement in response to L-dopa administration was achieved in 2 NHP treated with AAV-NULL without inducing dyskinesias. However, the AADC-treated group developed dyskinesias in the first 5 days of treatment that persisted despite lowering the dose of Sinemet. Both groups had some degree of other adverse effects of L-dopa treatment such as hyperactivity, aggression, occasional apparent hallucinations and self-mutilation. (C and D) Eight monkeys, in which *diffuse* transgene expression (NULL or AADC; $n = 4$ in each group) was achieved, were subjected to a similar regimen of Sinemet CR for 7 weeks. No dyskinesias were observed in response to either acute or chronic L-dopa.